

Actuator Servos for Deformable Mirrors



Roger Svahn

IEA, Lund University

Lund Observatory, Lund University

Department of Automatic Control, Lund University

Actuator Servos for Deformable Mirrors

Roger Svahn

Supervisors: Torben Andersen and Gustaf Olsson

May 16, 2005

ABSTRACT

The Euro50 is planned to be largest telescope in the world and will use adaptive optics. The adaptive optics system needs to deform the telescope's secondary mirror. Actuators will introduce that deformation by pulling and pushing on the back of the mirror.

In this thesis a special type of actuator is studied. The purpose is to produce an inexpensive actuator with a low power consumption, using a voice coil as the actuator. The special aspect of this actuator design is that it does not have a stiff connection to the mirror. Normally it is desirable to have a stiff connection to be able to make a good controller. In this case a vacuum cup with very low stiffness is used. To accomplish this, a Linear Variable Differential Transformer (LVDT) is used to measure the movement of a voice coil. The information from the LVDT is used in an inner control loop, controlling the movement of the voice coil. By knowing the properties of the vacuum cup and using that information, it is possible to make a virtual force actuator. A positive feature with this design is that the assembling and disassembling of the actuators will be much easier than for actuators rigidly attached to the deformable mirror. The electronic drive circuit required for the voice coil has been designed as well as a thermal protection circuit, preventing overheating of the coil. A model of the actuator has been created and verified. By using the model, a controller has been designed. Experiments showed that cross talk in the LVDT electronics and noise picked up by the LVDT made the controller unusable. A couple of ideas for solutions to the problem is discussed. One of the solutions, using an observer to estimate the velocity of the voice coil, has been simulated and the results seem promising.

CONTENTS

1. <i>Introduction</i>	1
1.1 The Euro50 Telescope	1
1.2 Adaptive Optics	2
1.3 Deformable Mirrors	2
1.4 Actuators	3
1.5 Voice Coil Actuator with Vacuum Cup	4
1.6 Related projects	5
2. <i>Problem Formulation</i>	6
3. <i>Overview of the System</i>	7
4. <i>Actuator</i>	8
4.1 Actuator Principle	8
4.2 Voice Coil	8
4.3 Linear Variable Differential Transformer	10
4.4 Vacuum Cup	10
5. <i>LVDT Electronics</i>	12
5.1 Possible Improvements of the Electronics	14
6. <i>Actuator Properties</i>	15
6.1 Coil Inductance	15
6.2 Thermal Time Constant	16
6.3 Stiffness of the Vacuum Cup	17
6.4 Signal Conditioner Output	17
6.4.1 Noise	19
7. <i>Drive circuit</i>	20
7.1 Power Amplifier	20
7.2 Temperature Control Circuit	22
7.3 Level Detector	22

8. <i>Modeling</i>	26
8.1 Actuator	26
8.2 Actuator and Vacuum Cup	27
8.3 Actuator, Vacuum Cup and Mirror	27
9. <i>Model verification</i>	31
10. <i>Controller</i>	35
10.1 Analog Implementation	35
10.2 Alternative Filter	38
10.3 Sallen-Key Filter	40
11. <i>Potential use of an Observer</i>	42
12. <i>Conclusion and Suggestions of Future Work</i>	46
<i>Bibliography</i>	48

1. INTRODUCTION

1.1 The Euro50 Telescope

There are several ongoing projects in Europe for Extremely Large Telescopes (ELTs). Lund Observatory in Sweden is involved in one of these projects called Euro50. Euro50 is designed with a 50 meter primary mirror and a 4 meter secondary mirror. Both mirrors will use adaptive optics. The reason for building a telescope that large is that the larger diameter, the better light collection capability. Pictures with higher resolution gives the possibility to discover new phenomena and get a better understanding of the universe. Building a telescope of that size on the Earth would be a waste without adaptive optics since the earth's atmosphere distorts the light and makes it impossible to get high resolution observations if no corrections are made.



Fig. 1.1: Comparison of size. Left: Jumbo jet (Boeing 747-200), Right: The Euro50 (from [2]).

There are two different designs for extremely large telescopes, the primary mirror can be spherical or aspherical. Both have their advantages and disadvantages. The spherical primary mirror can be made of many identical segments and is therefore less expensive than the aspherical where every segment has to be specially made. The major disadvantage is that the spherical primary mirror causes strong spherical aberration that has to be corrected

with 2-4 additional mirrors. The aspherical primary mirror design has the advantage that it only needs two mirrors and the adaptive optics can be easily integrated into the telescope. The reason for making a large telescope is to collect as much light as possible and to get a good resolution, but the intensity of the light decreases by $\approx 10\%$ for every extra reflection. In the spherical design there are 3-5 mirrors which lead to unnecessary light losses.

1.2 Adaptive Optics

When the light travels through space there is nothing to refract the light. All the light traveling from its source has the same path and has the same phase i.e., the wavefronts are planar. But when the light passes through the atmosphere it refracts differently depending on the density of the layer in the atmosphere and this will result in wavefront aberrations. The refraction index depends on mixing of air with different temperature, humidity and pressure [4]. Powerful winds of high speed create turbulence in the atmosphere layers. The wind in these layers involve frequencies up to about 500Hz. When the light reaches the telescope it has a wavefront that is not plane leading to pictures with poor resolution. Adaptive optics is used to compensate for the non-planar wavefront and achieve a good resolution. By deforming the secondary mirror on the telescope with very high precision, the unplane wavefront can be compensated. The deformation is made by applying many actuators on the back of the mirror and letting them push and pull to deform the mirror with high accuracy. With 3000 actuators and 3500 sensors, a deformation of tens of micrometers and an accuracy of nanometers, the requirements for the adaptive optics system are high. The adaptive optics will also need to react with a bandwidth of 500 Hz. By using adaptive optics the resolution can be almost as good as if the telescope would be placed outside the atmosphere.

1.3 Deformable Mirrors

The adaptive optics need deformable mirrors (DMs) for correction of wavefront aberrations. There are different kinds of deformable mirrors. The primary and the secondary mirrors on the telescope can be used as deformable mirrors or smaller mirrors can be placed near the focus of the light. In the first alternative the secondary mirror will correct mainly for the light aberrations caused by the atmosphere and the primary will adjust the focus. The alternative with the small deformable mirrors involves many extra relay mirrors to transmit the light to the mirrors. For each reflection the light loses

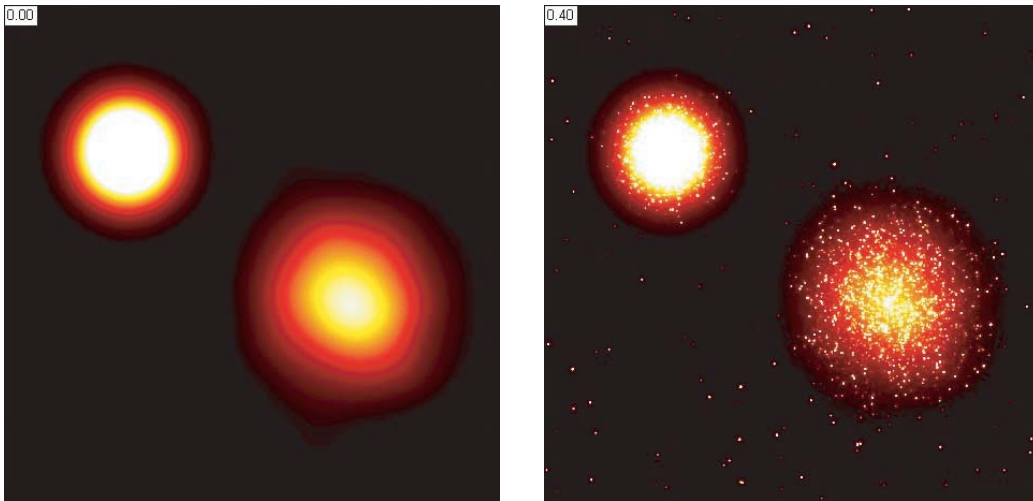


Fig. 1.2: Simulation of the effect of adaptive optics in the Euro50². Left: Image without adaptive optics. Right: Using adaptive optics. Simulation: Ralph Snel, Lund Observatory.

up to 10% of its intensity. This counteracts the whole purpose of building an ELT. When the adaptive optics uses the primary mirror together with the secondary, the number of mirrors can be decreased, thereby avoiding loss of intensity. A drawback with this technology is that the control of the primary and secondary mirrors are far more advanced. The controller needs to deal with eigenfrequencies within the bandwidth of the controller. When using micro deformable mirrors the eigenfrequencies of the mirror are much higher and most of them are far beyond the controller bandwidth.

1.4 Actuators

Some solutions with different actuators have been tested using for example piezoelectric, magnetostrictive and electrostrictive materials [7]. A piezoelectric material changes its length due to changes in the electric field, i.e., by applying a voltage one can control both the direction and the amplitude. The material normally used for deformable mirrors (DMs) is PZT (lead zirconate titanate). The PZT has initially randomly oriented dipoles and has to be poled to get the piezoelectric effects. The deformation is linear but has a hysteresis between 10% and 20%. A positive feature is that it has

² The value in the upper left corner is strelh ratio. A typical value for the Euro50 will be in the range of 0.3-0.5, see [2]

a wide temperature range but the disadvantage is that the material has a rather high hysteresis and because the material is poled it loses sensitivity over time. The magnetostrictive actuator uses ferromagnetic materials that responds to changes in the magnetic field. With a special alloy it is possible to get magnetostrains comparable to current piezoelectric and electrostrictive materials. The actuator works over a wide temperature range but has a relatively high hysteresis around 20%.

When electrostrictive actuators are exposed to an electrical field, the positively and negatively charged ions separate and change the dimensions of the cell which results in an expansion of the material. The relationship between the voltage and the expansion is quadratic but that problem is not as serious as the temperature sensitivity. At a temperature of -10°C the sensitivity value reaches maximum and is twice the size compared to 25°C . The hysteresis also changes with temperature from 1% to 15%.

A drawback with all these actuators is that they have quite a high power consumption and will require some kind of cooling system. Independently of which of these material is used, it must have a very stiff connection to the mirror. The material has to be glued on and mounted quite permanently. The Euro50 will use at least 3000 actuators and the assembling would be quite difficult with these actuators. If or when an actuator needs to be replaced, this will be a problem too.

Using a voice coil will give an actuator with rather low power consumption and a larger stroke. It is also in comparison both inexpensive and easy to implement. The larger stroke can be used for tilt function of the mirror. The tilt correction with small amplitude and high bandwidth can be taken care of by the actuators while control of the whole mirror cell takes care of the larger slow corrections, see also [12]. The other actuators described are intrinsically stiff but the voice coil has no stiffness. A stiff actuator would be easier to control because resonance frequencies of the mirror will become much higher (above 1 kHz).

1.5 Voice Coil Actuator with Vacuum Cup

In this master thesis we look at the possibility of using a special kind of actuator. This actuator uses a vacuum cup as the connection between the mirror and the voice coil. As previously stated it gives a connection with a very low stiffness. The actuator uses a voice coil to get the movement and an LVDT¹ to measure the movement of the rod pushing the mirror. The vacuum cup works as a spring. A movement of the rod will strain the

¹ LVDT=Linear Variable Differential Transformer

spring and give a smaller movement of the mirror. The LVDT can measure with a precision of a few micrometers but the mirror has to be controlled with a precision of tens of nanometers. With an internal control loop in the actuator, the movement of the rod can be controlled and the actuator will work as a virtual force actuator. With this solution it is easier to mount and replace the actuators since they are only connected with a vacuum cup.

1.6 Related projects

Two other theses on the adaptive optics on Euro50² have been done at Lund Observatory in parallel with this thesis. One of these projects concerned a controller that can control the whole mirror surface by using all of the 3000 actuators [5]. The other has been the control of the position of the whole mirror cell. The mirror cell will be placed about 60 meters above ground and weighs about 700kg. The mirror cell needs to keep its position with a precision of micrometers. Both projects show quite difficult control problems.

² For more information about Euro50 visit <http://www.astro.lu.se/~torben/euro50/>

2. PROBLEM FORMULATION

The purpose of this thesis is to:

- Set up an experiment platform for the actuator.
- Design a drive circuit for the voice coil.
- Make a simulation model of the actuator.
- Design an analog control loop.
- Measure open and closed loop frequency responses for the actuator.
- Connect the actuator to a small test mirror and verify the performance using an interferometer.

The goal is to get an actuator that can deform a mirror cell with $\approx 20\mu m$ with an accuracy of $\approx 20nm$. This has to be made with a bandwidth of at least 500Hz, preferably 1000Hz.

3. OVERVIEW OF THE SYSTEM

The system has been divided into four parts: controller, drive circuit, actuator and LDVT electronics. Each part is described in a separate chapter. The block diagram in Fig. 3.1 gives a general view of the system setup. The control circuit filters the reference error signal and feeds it to the drive circuit. The drive circuit is needed to get a sufficient current to drive the voice coil in the actuator. Included in the drive circuit is a thermal protection circuit, which will limit the current to the voice coil, to prevent overheating of the coil. The voice coil performs the stroke of the actuator rod. The movement of the rod is measured by an LVDT, which works as a electromechanical transducer i.e., it transforms a mechanical movement of the rod to a voltage output. The LVDT output is finally transformed in the LVDT electronics, to a DC-voltage proportional to the movement of the rod, before it is fed back to the controller.

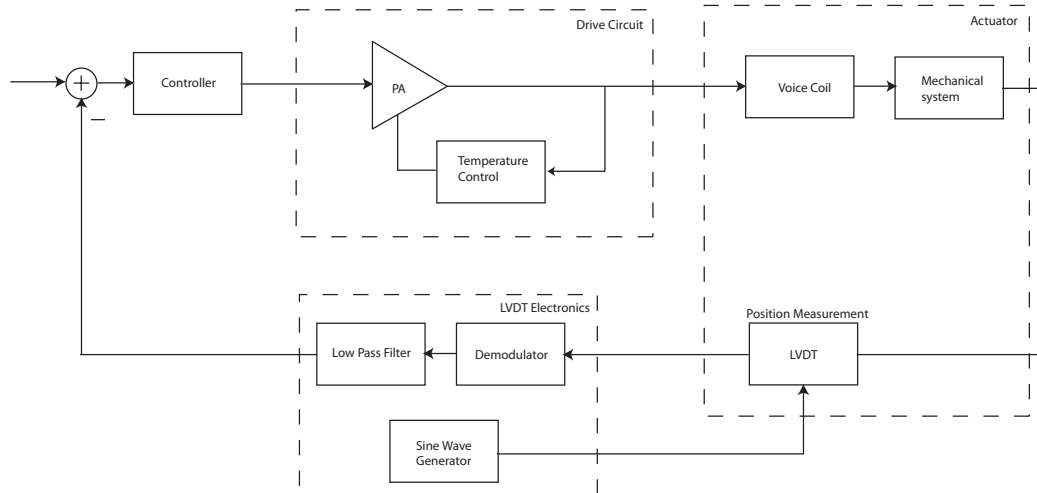


Fig. 3.1: Block diagram of the complete system

4. ACTUATOR

4.1 *Actuator Principle*

The actuator, which is a prototype, consists of a voice coil that will give the force and an LVDT measuring the movement (see Fig. 4.1). The two parts are connected with an rod. The rod is made of two brass connection pins, a core of a magnetic material for the LVDT and a connector where the vacuum cup is placed (see Fig. 4.2). The LVDT is placed between the voice coil and the vacuum cup. It would be desirable to switch the location of the voice coil and the LVDT, but this was not possible because of the construction. The voice coil has a low power consumption, is easy to integrate and is rather inexpensive which is why it was chosen in this application. Unfortunately the voice coil is not intrinsically stiff, which would be desirable. Instead of trying to get a stiff connection to the mirror, the connection is made with a vacuum cup, which also has low stiffness. The LVDT is used to measure the movement of the actuator. An inner loop in the actuator uses that information to control the movement. The voice coil has only an accuracy in the region of micrometers but the mirror position should have an accuracy of nanometers. This is where the vacuum cup's lack of stiffness can be utilized. The vacuum cup can be approximated as a spring that gets tightened when applying a force. The voice coil creates a force and moves a couple of micrometers, the spring gets tightened and will deform the mirror much less. By using a controller for the movement of the rod it is possible to control the force, resulting in a virtual force actuator.

4.2 *Voice Coil*

A voice coil is normally used in for example a loudspeaker to create sound. A coil of wire is placed in a gap of a core of magnetic metal. When applying a current to the coil a magnetic field arises. The electromagnetic field interacts with or counteracts with the field of the permanent magnet. This will create a force with a direction determined by the sign of the current. The voice coil used is one of few prototypes made by a company, but it will be produced

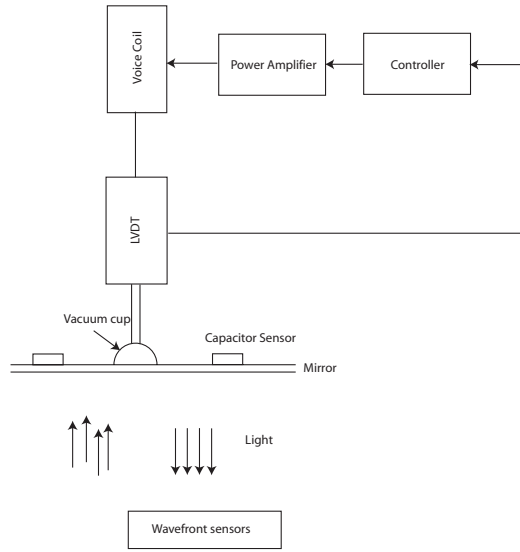


Fig. 4.1: Principle of the actuator.

in bigger quantity. Most of the information about it can be found in the datasheet published by the company. The information is shown in Table 4.1.

Tab. 4.1: Data for the Voice coil

Winding Constants	Symbols	Values
DC Resistance	R	5.4Ω
Voltage@ F_P	V_P	$9.72V$
Current@ F_P	I_P	$1.8A$
Force Sensitivity	K_F	$2.33 N/A$
Inductance	I	$100mH^1$
Actuator Parameters	Symbols	Values
Peak Force	F_P	$4.2N$
Actuator Constant	K_A	$1N/\sqrt{W}$
Power@ F_P	P_P	$17.5W$
Stroke		$\pm 2 mm$
Thermal Resistance of Coil	θ_{TH}	$41 ^\circ C/W$
Maximum allowable Coil Winding Temp	Temp	$155^\circ C$
Weight of Coil Assembly	WT_C	$1.2g$
Total Weight	W_{TT}	18.5

¹ Undefined in datasheet, measured to $\approx 100mH$.

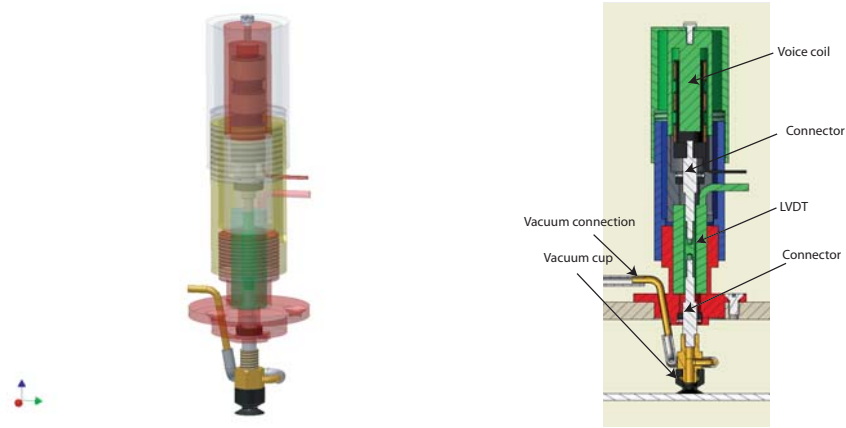


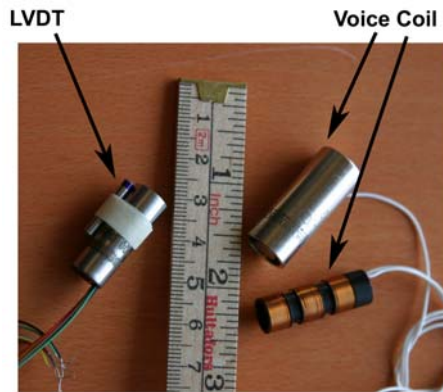
Fig. 4.2: Mechanical drawing of the actuator.

4.3 Linear Variable Differential Transformer

A Linear Variable Differential Transformer (LVDT) is an electromechanical transducer. The LVDT input is a mechanical displacement of the core, and the output is an AC-voltage proportional to the core position. The LVDT, of type "CD 375-100", is used with an electronic circuit of type "DCM-1000". The LVDT consists of three coils with a moving magnetic core inside the coils. The middle coil is the primary and it works as a transmitter. The other two coils are secondary coils and work as receivers. The receivers are at the same distance from the transmitter and are connected with reverse polarity. The two signals added make up the output. When the core is in the middle of the two coils the circuit is balanced and the output signal is zero. As the core makes a slight movement, the electrical field for the secondary coils changes and creates unbalance. The excitation signal used by the transmitter coil is produced by the LVDT electronics, which also converts the received signal to a DC-voltage output (see Chapter 5).

4.4 Vacuum Cup

The vacuum cup in the first experiments was a sample from a company and made of nitrile. The stiffness of the cup is important to get the right performance of the actuator; with a very stiff cup a large force will give a small movement of the actuator rod. A small movement demands less power from the voice coil. Since the accuracy of the actuator depends on the measurements of the LVDT it is important that the LVDT can measure the movement. Therefore the movement can not be too small and the stiffness



Specifications LVDT CD 375-100

Input Voltage.....	3Vrms
Input Frequency.....	2.5 - 3.0 kHz
Linearity Error.....	< $\pm 0.25\%$ of FRO
Vibration Tolerance.....	20 g to 2 kHz
Nominal Range.....	± 2.5 mm
Sensitivity.....	63 mv/V/mm
Impedance.....	340 Ω

Fig. 4.3: Photography of the LVDT and the voice coil.

can not be too large, this is all a trade-off. After the experiments on the nitrile vacuum cup it became clear that the cup was too stiff (see more in Chapter 9). A new cup was made out of silicone rubber. The new cup had a stiffness of 11.8 kN/m instead of the nitrile cup with the stiffness of 30 kN/m.

5. LVDT ELECTRONICS

The LVDT electronics work as a drive circuit as well as a signal conditioner for the LVDT. The oscillator, included in the electronic circuit, provides the excitation signal for the LVDT (see Fig. 5.1). The excitation signal is amplified before it is fed to the primary coil of the LVDT. The two receiver coils receive the signal transmitted by the primary coil. When the rod is moving, the electrical field changes and a signal with the same frequency as the movement arises. That signal is amplified before it is fed into the demodulator together with the excitation frequency. When the rod is kept still the output of the demodulator is just the excitation signal rectified. When the rod makes a slight movement, there is an amplitude change in the two receiver signals and the circuit gets unbalanced. The shift depends on the direction of the movement and causes an additional DC-signal at the output. The sign of the DC-signal is related to the direction of the rod. The demodulator output is fed to a Sallen-Key¹ Butterworth low-pass filter to get rid of the superposed frequency, which is twice the excitation frequency. The output is a nearly ripple free $\pm 10V$ DC-voltage output.

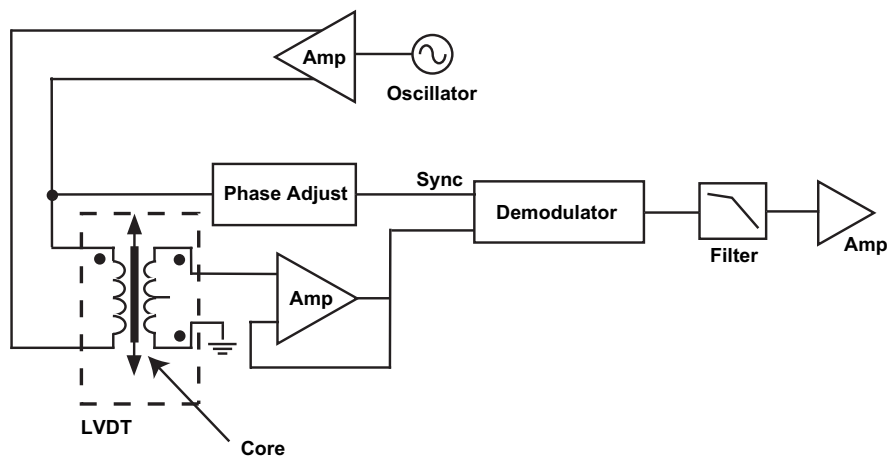


Fig. 5.1: The principle of the LVDT

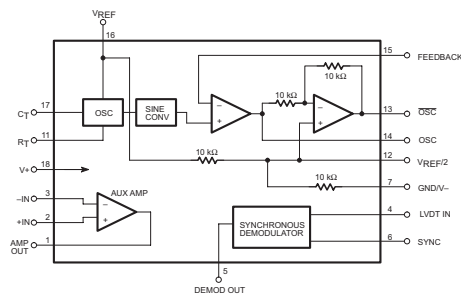
¹ Read more about Sallen-Key low-pass filters in Section 10.3

The LVDT electronics used is a standard circuit called "DCM-1000" and has not been designed especially for this application. The excitation frequency can be altered between three frequencies (3kHz, 5kHz and 10kHz). In the instruction manual [8] the bandwidth for the low-pass filter is denoted to 250 Hz. That bandwidth has been modified by the manufacturer and the new bandwidth is unknown. Since a bandwidth of 500-1000 Hz for the actuator is desirable, the excitation frequency of 10 kHz seems too small. Information about the circuit design was not available since the only enclosed document was the instruction manual. By examining the circuit it could be seen that an integrated circuit called NE5521 was used as the signal conditioner. According to the datasheet [10] it is possible to increase the excitation frequency to maximally 20 kHz. This modification can be made by replacing a capacitor C_T and using the equation

$$OSC\ frequency = \frac{V_{REF} - 1.3V}{V_{REF} * (R_T + 1.5e3) * C_T}, \quad R_T = 18k\Omega \quad (5.1)$$

for calculating the value, see [10]. According to the specification the input frequency of the LVDT is specified to between 2.5kHz-3kHz (see previous Chapter). That frequency would be too low for this application but the LVDT was the only one available for this project. A 20 kHz excitation frequency was chosen, even if it is outside the specified range for the LVDT. In experiments in the future it is possible that a new LVDT, that can tolerate higher excitation frequencies, will be purchased.

In the application notes of NE5521 [11] the use of an active filter using the uncommitted amplifier is described. Looking more closely on the circuit it showed that the same type of filter has been used as the one discussed in [11]. After locating the filter, the bandwidth could be measured to 10 Hz. This bandwidth is far too low for the application in mind. The filter was then replaced with a Butterworth low-pass filter with a cut-off frequency at 4 kHz. The filter could affect the control of the actuator, but it is necessary to damp the 40 kHz signal (twice the excitation frequency).



Specifications signal conditioner
 Input Voltage..... $\pm 15V$ DC
 Input Current..... $50mA$
 LVDT Excitation Volt... $3 V_{rms}$
 LVDT Excitation Freq... $3kHz, 5kHz$ or $10kHz$
 Output Voltage..... $\pm 10V$
 Output Current..... $5mA$
 Frequency Response^a..... $-3dB$ at $250Hz$
 Output Ripple..... $<10mV_{rms}$

Fig. 5.2: Schematic of the NE5521 signal conditioner circuit (from [11]).

^a Cut-off frequency of filter later changed to $4kHz$

5.1 Possible Improvements of the Electronics

The LVDT electronics used is a commercial circuit and the knowledge about the design is limited. As discussed in Chapter 6.4.1 there is some problem with crosstalk on the circuit. Minimizing the crosstalk is necessary for a good control of the actuator. To minimize the crosstalk it is important to know all of the building blocks of the circuit, therefore a new circuit will be produced. When designing the new circuit a different integrated circuit will be used for the demodulation. The new circuit, called AD698, uses a different technique when demodulating which is more exact.

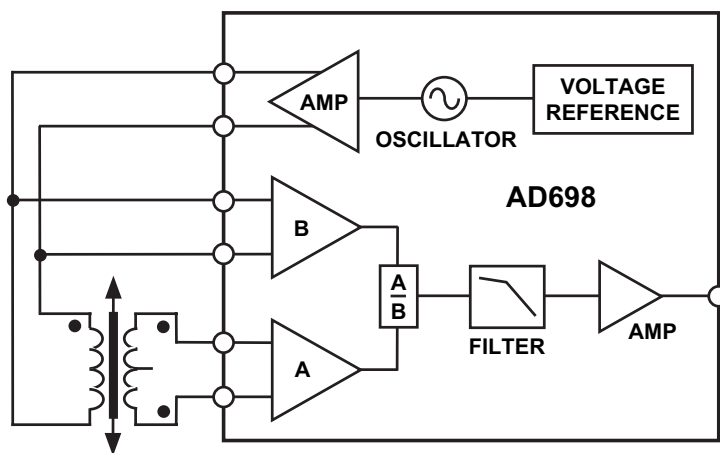


Fig. 5.3: Functional Block Diagram for circuit AD698 (from [3]).

6. ACTUATOR PROPERTIES

The voice coil used as the actuator was a prototype and there was no information about it available. Therefore some experiments needed to be done to determine the inductance and the thermal time constant of the coil. The properties of the vacuum cup, that will connect the actuator to the mirror, was also unknown. Several different vacuum cups were later used but the first one was made of nitrile. To make a simulation model it was necessary to know the stiffness and the damping of the vacuum cup. The stiffness can be determined by an experiment where you measure the deformation under a static force. The experiment was just to get a rough estimation to be able to make a model and was just made for the first vacuum cup tested (see Chapter 6.3). There is no possibility to measure the velocity in the voice coil thus the damping was not tested. The damping can be calculated by using a Bode plot of the open loop function for the system. The amplitude of the resonance peak in that plot is proportional to the damping in the vacuum cup.

6.1 Coil Inductance

The inductance of the voice coil was not specified in the data sheet [9]. Therefore it had to be measured. A resistance ($R=220\Omega$) was connected in series with the voice coil. The voice coil's internal resistance is 5.4Ω but with the connecting cables it was measured to $R_L = 5.9\Omega$. The resistance voltage drop as well as the coil voltage drop were measured. The inductance could then be calculated with Equation 6.1. This experiment was made for different frequencies but the result varied and therefore the inductance was determined for $f=500$ Hz since that is the desired bandwidth for this application. The inductance was calculated through the measurements to $L=100\mu\text{H}$.

$$V_L = V_{total} \left(\frac{j\omega L + R_L}{R + R_L + j\omega L} \right) \quad (6.1)$$

6.2 Thermal Time Constant

The thermal time constant is important to know since the actuator needs to use the peak force of the voice coil. When continuously applying a current, corresponding to the peak force, the coil will get heated above safe operating temperature. There is no temperature sensor in the coil winding and therefore it is necessary to estimate the temperature. To be able to do this, the thermal time constant is determined through experiments. With a constant current applied to the coil, the resistance increases with time since the temperature in the winding increases. A current was applied to the voice coil during ten minutes and after that time the power was disconnected. The resistance was measured as the temperature decreased. When the resistance reached its original value the measurements were interrupted. The result is plotted in Fig. 6.1. The time constant in that plot corresponds to the thermal time constant ($\approx 70\text{s}$).

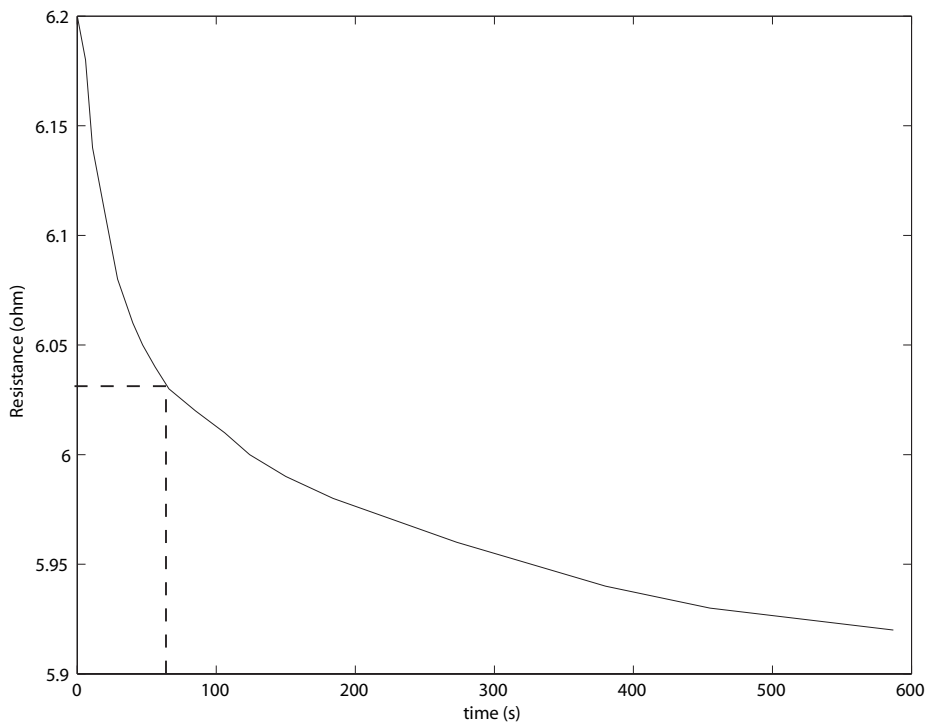


Fig. 6.1: The resistance in the voice coil after disconnecting a constant current source.

6.3 Stiffness of the Vacuum Cup

To determine the stiffness of the rubber cup a DC current was applied to the voice coil. The mirror's movement was measured externally with a dial indicator and the movement of the voice coil was measured with the LVDT. The difference between the two measurements is the deformation of the vacuum cup. The force sensitivity of actuator is 2.33 N/A which in this case will give $F = 0.85N$, with the current 0.365A. Equation 6.2 below gives the stiffness 10.7 kN/m. This experiment was made for a the nitrile cup.

$$F = k \cdot \Delta, \text{ k=stiffness, } \Delta=80\mu\text{m} \quad (6.2)$$

6.4 Signal Conditioner Output

The signal conditioner circuit gets a modulated signal containing the excitation frequency and the frequency of the reference signal. The signal conditioner demodulates the signal and gives a signal with twice the excitation frequency as output. That frequency is filtered by a couple of Sallen-Key low-pass filters, after these filters the output signal should contain nearly only a signal with the same frequency as the reference signal.

A spectrum analysis was made of the output signal, the result can be seen in Fig. 6.2. The power spectrum shows large contributions at 5kHz, 15kHz, 20kHz and 40kHz. The driving frequency in this experiment was 5kHz and this signal can be observed in the power spectrum. The signal of 40kHz is twice the excitation signal and has been filtered in two Butterworth low-pass filters so it should be more damped than it is. The excitation signal of 20kHz has been rectified in the demodulator and should not be visible at the output.

It seems that the 20kHz signal is caused by cross talk in the signal conditioner circuit. The oscillator providing the 20kHz signal is located on the same circuit board as the demodulator. This could cause interference with the output and thereby explain the 20kHz signal in the power spectrum plot. The 15kHz signal is a consequence of the remaining 20kHz signal. Amplitude modulation of the 5kHz signal and the 20kHz signal results in a 15kHz signal and a 25kHz signal. When amplitude modulating a signal, the amplitude A of a carrier wave $v_c(t) = a \cdot \cos(\omega_c t)$ varies with a baseband signal $v_m(t) = a \cdot \cos(\omega_m t)$ so that $A = K + v_m(t)$ where K is the amplitude of the unmodulated signal. The equation can be written as

$$v_c(t) = A \cos(\omega_c t) = [K + a \cdot \cos(\omega_m t)] \cos(\omega_c t) = K [1 + m \cdot \cos(\omega_m t)] \cos(\omega_c t) \quad (6.3)$$

where $m = \frac{a}{K}$ is the degree of modulation. By using the trigonometric formula $\cos(\alpha)\cos(\beta) = \frac{1}{2} [\cos(\alpha - \beta)] + \frac{1}{2} [\cos(\alpha + \beta)]$ the result can be written as

$$v_c(t) = K \cos(\omega_c t) + \frac{Km}{2} \cos[(\omega_c - \omega_m)t] + \frac{Km}{2} \cos[(\omega_c + \omega_m)t] \quad (6.4)$$

As the equation shows, the modulated signals has the frequencies 15kHz, 20kHz and 25kHz¹. The presence of the 15kHz signal implies that the cross talk in the circuit appears before the demodulator. The 25kHz signal is however not visible in the power spectrum plot. This could be due to the low-pass filter on the signal conditioner circuit that attenuates signals over 4kHz. The frequency that is a result of the modulation can be a problem when the reference signal reaches half the excitation frequency. At that point there are two contributions to the 10kHz signal.

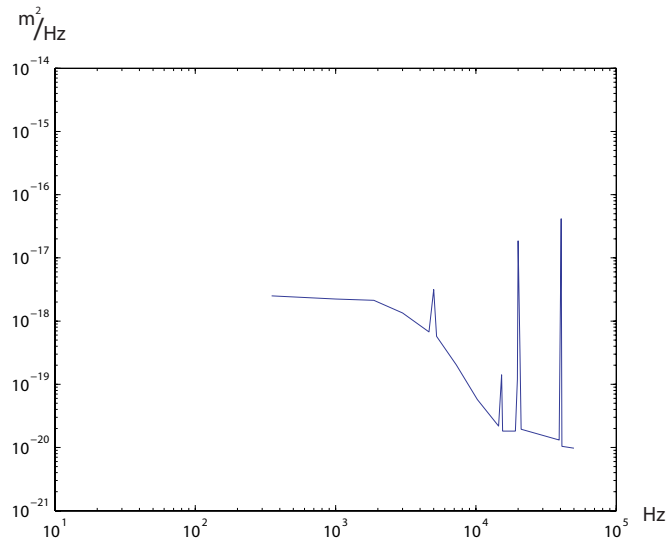


Fig. 6.2: Power spectrum density of LVDT electronic output. A 5kHz reference signal used as input.

¹ $\omega_c = 20\text{kHz}$ and $\omega_m = 5\text{kHz}$

6.4.1 Noise

The noise seen by the LVDT electronics was analyzed by measuring the output when the input was connected to ground. The signal observed at the output is then the noise. It is important that the noise does not interfere with the measurements of the movement. The LVDT measures the movement of the voice coil with high accuracy. The signals from the LVDT are quite small and noise from the electronics will be interpreted as a movement. A power spectrum was made of the output from the circuit and the result is shown in Fig. 6.3. The signals seen in the plot are mostly mains noise and its higher order harmonics. Except for those signals there is a great contribution of a 20kHz signal. This signal is of course the oscillator signal that gives the excitation frequency for the LVDT. The signal should not be visible. The fact that it is visible again indicates that there is cross talk on the LVDT circuit.

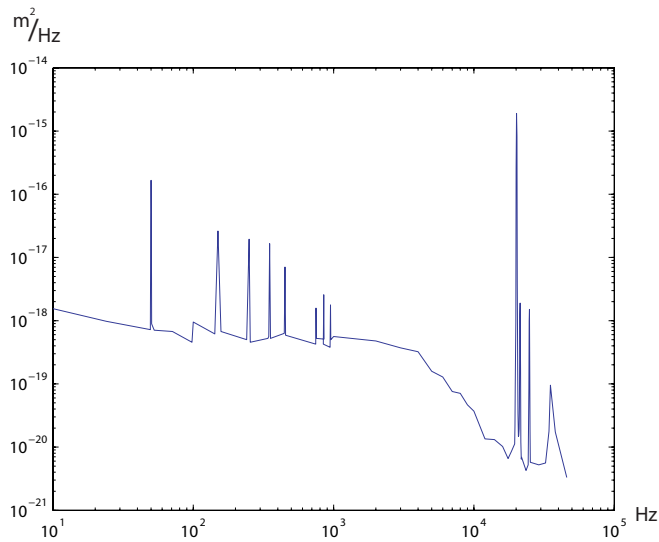


Fig. 6.3: Power spectrum density of the LVDT electronics without any input signal.

7. DRIVE CIRCUIT

The force of the voice coil is proportional to its input current. The current demanded of the voice coil requires a power amplifier, which is the main part of the drive circuit. The voice coil consists of a coil made of very thin copper wire, and applying the maximum current for a long period of time will for sure destroy the coil windings. To avoid this, a thermal control circuit is included in the drive circuit (see Fig.7.1). The complete circuit consists of the power amplifier, an additional amplifier, multiplier, polyester capacitor and a level detector. As output from the power amplifier circuit is a voltage proportional to the current through the coil. This voltage is then amplified to get the right input to the multiplier. After squaring, the signal is proportional to the power dissipated in the coil. The multiplier has a current output, which is used to charge the following polyester capacitor. The time it takes for the capacitor to get charged, the electrical time constant, is chosen to correspond to the thermal time constant of the coil. Using this principle, the capacitor will be fully charged when it is time to decrease the current through the coil for safety reasons. The capacitor voltage is then fed to a level detector, which feeds its output back to the current limiter input of the power amplifier.

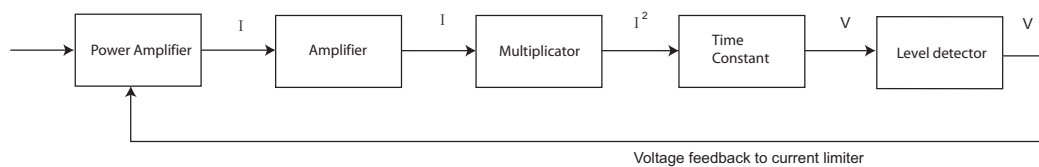


Fig. 7.1: Block diagram of the drive circuit with temperature control.

7.1 Power Amplifier

The voice coil is current controlled and gives the peak force at 1.8A. That current is also the maximum current allowed for the voice coil. A power amplifier is needed to supply the demanded current and a current control is desirable for safety reason. The amplifier chosen is the OPA548 which has

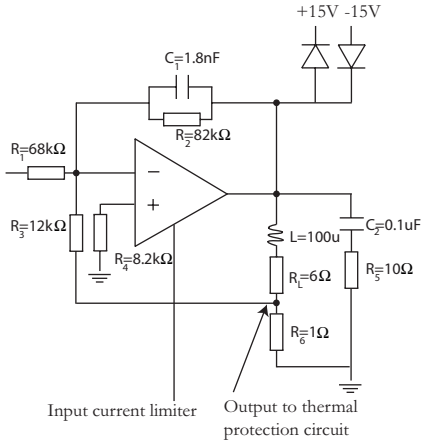
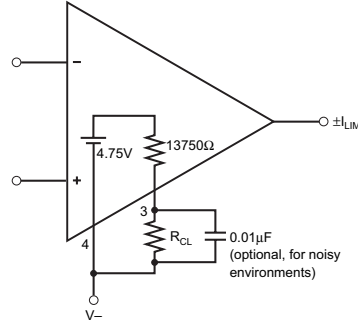


Fig. 7.2: Power amplifier schematic, where L and R_L are the inductance respective the resistance of the voice coil.



OPA548 CURRENT LIMIT: 0 to 5A

DESIRED CURRENT LIMIT	RESISTOR ⁽¹⁾ (R_{CL})	CURRENT (I_{SET})	VOLTAGE (V_{SET})
0A	I_{LIM} Open	0μA	$(V-) + 4.75V$
1A	57.6kΩ	67μA	$(V-) + 3.8V$
2.5A	14.7kΩ	167μA	$(V-) + 2.5V$
3A	10kΩ	200μA	$(V-) + 2V$
4A	4.02kΩ	267μA	$(V-) + 1.1V$
5A	I_{LIM} Connected to $V-$	333μA	$(V-)$

Fig. 7.3: Adjustable Current Limit for circuit OPA548(from [13]).

a current limit, controlled with an external resistor. Since the voice coil can not manage more than 1.8A, a fixed, upper current limit is set to this value. The current limiter (see Fig. 7.3) uses a voltage source inside the amplifier. By choosing an external resistor, a voltage divider is made together with the internal resistor ($R_{internal} = 13750\Omega$). By looking in the table in Fig. 7.3 it can be seen that the sum of the negative power supply voltage and the voltage over external resistor is equal to V_{set} . When the voltage $V_{set} = (V-) + 4.75$, in this case equal to $-10.25V$, the current limiter will completely cut the current at the output. The size of the resistance is calculated using Eq. 7.1 according to the data sheet of the amplifier [13].

$$R_{CL} = \frac{15000 * 4.75}{I_{LIM}} - 13750\Omega \Rightarrow R = 26k\Omega \quad (7.1)$$

Since the load of the amplifier is an inductance (the voice coil) a load current could return to the amplifier and make the output voltage exceed the supply voltage. To prevent this two diodes are connected from output to $\pm 15V$ as shown in Fig. 7.2. The inductive load could also cause output instability. According to [13] this can be solved with a resistance and a capacitor connected in parallel to the inductive load. In the same datasheet the problem of disturbances from the power supply is discussed. The power supply can cause instability in the amplifier, but it can be taken care of with capacitors as shown in Fig. 7.4. The power amplifier is used as a voltage inverter with a current feedback loop. The input voltage of the amplifier

is $\pm 10V$ with an amplification corresponding to a voltage that will give a $\pm 1.8A$ current through the load.

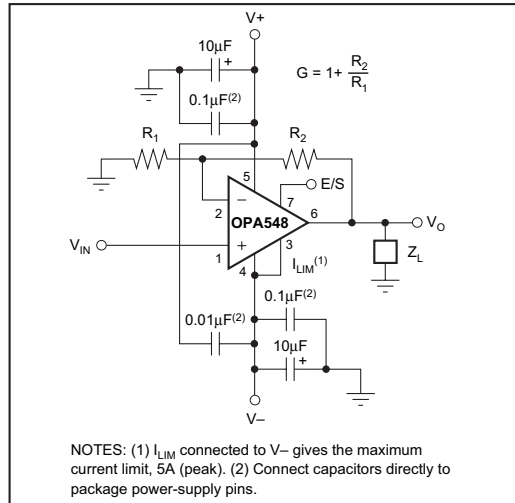


Fig. 7.4: Basic circuit connections (from [13], Figure 1).

7.2 Temperature Control Circuit

The maximum current allowed through the voice coil is 1.8A but it can only manage a continuous current of 0.8A without getting overheated. Since there is no temperature sensor in the coil it is necessary to estimate the temperature to achieve a thermal protection. A resistance of 1Ω is connected between the coil and ground to measure the current through the coil. The voltage over the resistance is proportional to the current. This voltage is scaled with a voltage inverter to fit the following multiplier. The reason for squaring the current is to get a value proportional to the power dissipated in the voice coil. The multiplier has a controllable output current, which charges a capacitor that has the same electrical time constant as the thermal time constant of the coil. The capacitor is dimensioned so that it will be charged with 5V when the coil temperature is $155^\circ C$. The voltage is then amplified with the amplification -1 before a level detector.

7.3 Level Detector

The level detector is a voltage-inverter with two added voltages at the input. One of the voltages is $+15V$ and the other one is the voltage from

the polyester capacitor. The voltage from the capacitor has gone through a voltage-inverter so it is negative. The input from the positive power supply voltage has a variable amplification A_{f1} chosen by the variable resistor. The other input is negative and has the amplification A_{f2} . When adding these two voltages the output will be less than $-15V$, when the capacitor is uncharged (see Equation 7.3). Since the amplifier output is limited to $-15V$ the output will be constant $-15V$ until the capacitor is charged. When the capacitor is charged the input voltage decreases, since there is an addition of the positive voltage $+15V$ and the negative voltage from the capacitor. As the input voltage decreases the output will increase. The variable amplification is chosen to get the desired output value when the capacitor is charged with $5V$.

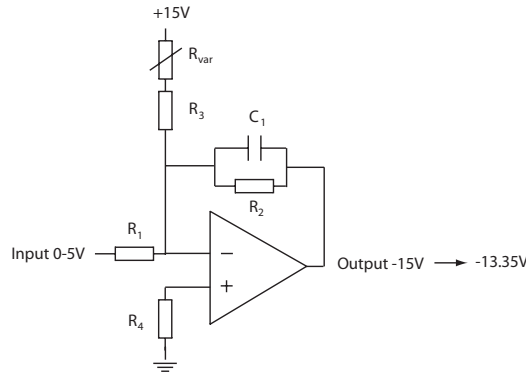


Fig. 7.5: Analog schematic of the level detector.

The output voltage is fed back as the input to the current limiter of the power amplifier. The voltage called V_{set} in Fig. 7.3 is the sum of the input voltage of the current limiter and the voltage over the external resistor. When V_{set} is $-10.25V$ the output of the power amplifier is limited to $0A$. The voltage over the external resistor is given by

$$V_{R_{CL}} = 4.75 \frac{26k\Omega}{13.75k\Omega + 26k\Omega} = 3.1V. \quad (7.2)$$

When the voltage $V_{set} = V_- = -15V$ the output is unlimited ($5A$). As the voltage V_{set} increases the current limit decreases. When the level detector output rise above $-15V$, V_{set} increases and the power amplifier output will be limited. The output of the level detector is chosen to $-13.35V$, when $5V$ input, since that gives $V_{set} = -13.35V + 3.1V = -10.25V$. This results in a zero output when the capacitor is charged with $5V$.

$$U_{output} = V_+ A_{f1} + V_{input} A_{f2} \quad (7.3)$$

$$A_{f1} = -\frac{R_3}{R_2}, \quad A_{f2} = -\frac{R_3}{R_1}$$

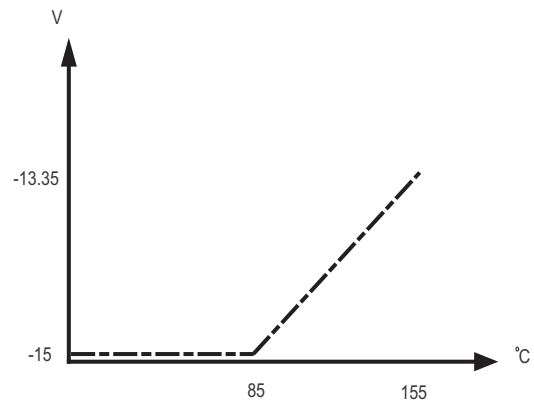


Fig. 7.6: Level detector.

8. MODELING

A mathematical model of the actuator connected to the mirror is needed to design a controller. The vacuum cup can be approximated as a spring with a damping. The model is seen in Fig. 8.1. The mass M_2 is the movable mass of the voice coil and M_1 is the mass of a mirror section. The constant for the stiffness of the vacuum cup is called K_2 and the damping for the same is called C_2 in the model. The mirror is as, an approximation, modeled as hexagon mirror segments, each one, held by six actuators, one in each corner, placed around the actuator in focus. The fixation of the mirror is then also modeled as a spring since the fixation consists of the actuators. That approximated spring is denoted as K_1 and C_1 . The real mirror is mainly held by the actuators but has also a fixed point in the middle. Except for these fixations the mirror will have an extra safety point of attachment, that will only be used when needed for safety reasons. The complete simplified model was split into three cases. The first case is if the actuator is disconnected from the mirror. The second case is if the mirror is stiff and third case is the complete model with the actuator connected and the deformable mirror. The reason to split the model in smaller parts is to get a simpler model in the beginning before designing a controller for the whole model, but also because it is important that the controller is stable for all three cases.

8.1 *Actuator*

The model of the actuator is made to make sure that the controller will be stable even if the mirror has no contact with the actuators. The actuators will normally have contact with the mirror at all times but some problem could arise, for example loss of vacuum. Since the mirror is excluded in this model there is now no spring active. The system is modeled just as a double integrator (see Eq. 8.1).

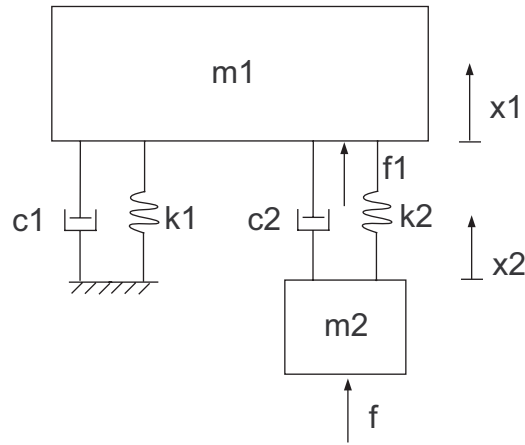


Fig. 8.1: Actuator and mirror model, where m_1 equals the mass of the mirror segment and m_2 the mass of the movable part in the actuator.

8.2 Actuator and Vacuum Cup

This model is derived for the case where the mirror is fixed. In this case the mirror model is used but since the mirror is stiff, the connections between the mirror and the other six actuators are excluded. The theoretical model of this system can be seen as two masses with a connection between them. The vacuum cup is that connection and can as an approximation be seen as a spring with damping (see Fig. 8.1).

8.3 Actuator, Vacuum Cup and Mirror

This model is the complete simplified model. This model is the same as the second one except in this case the mirror is deformable. Since the mirror is connected to the actuators around the one in the center you can say, as an approximation, that the mirror is connected to "ground" through a spring with damping (Fig. 8.1). The equation 8.1 has been transformed to state-space (see Eqs. 8.2 and 8.3) to describe the relationship for the two masses.

$$\begin{cases} \ddot{x}_1 m_1 = F_1 - k_1 x_1 - C_1 \dot{x}_1 \\ \ddot{x}_2 m_2 = F - F_1 \\ F_1 = (x_2 - x_1)k_2 + (\dot{x}_2 - \dot{x}_1)C_2 \end{cases} \quad (8.1)$$

$$\begin{aligned} \dot{x} &= Ax + BF \\ y &= Cx + DF \end{aligned} \quad (8.2)$$

$$\begin{pmatrix} \ddot{x}_1 \\ \dot{x}_1 \\ \ddot{x}_2 \\ \dot{x}_2 \end{pmatrix} = \begin{pmatrix} -\frac{C_1}{m_1} + \frac{C_2}{m_2} & -\frac{k_1}{m_1} + \frac{k_2}{m_2} & \frac{C_2}{m_1} & \frac{k_2}{m_1} \\ 1 & 0 & 0 & 0 \\ \frac{C_2}{m_2} & \frac{k_2}{m_2} & -\frac{C_2}{m_2} & -\frac{k_2}{m_2} \\ 0 & 0 & 1 & 0 \end{pmatrix} \begin{pmatrix} \dot{x}_1 \\ x_1 \\ \dot{x}_2 \\ x_2 \end{pmatrix} + \begin{pmatrix} 0 \\ 0 \\ \frac{1}{m_2} \\ 0 \end{pmatrix} \quad (8.3)$$

$$C = \begin{pmatrix} -C_2 & -k_2 & C_2 & k_2 \end{pmatrix}, D = 0$$

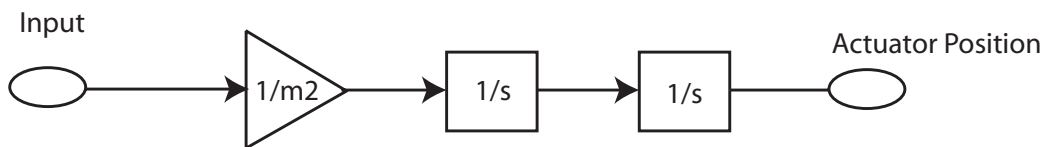


Fig. 8.2: Simulink model of Actuator.

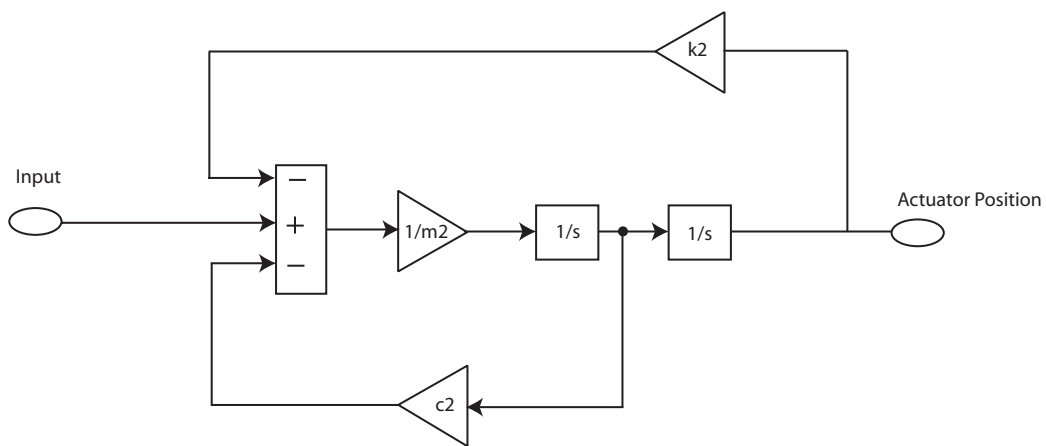


Fig. 8.3: Simulink model of Actuator and vacuum cup.

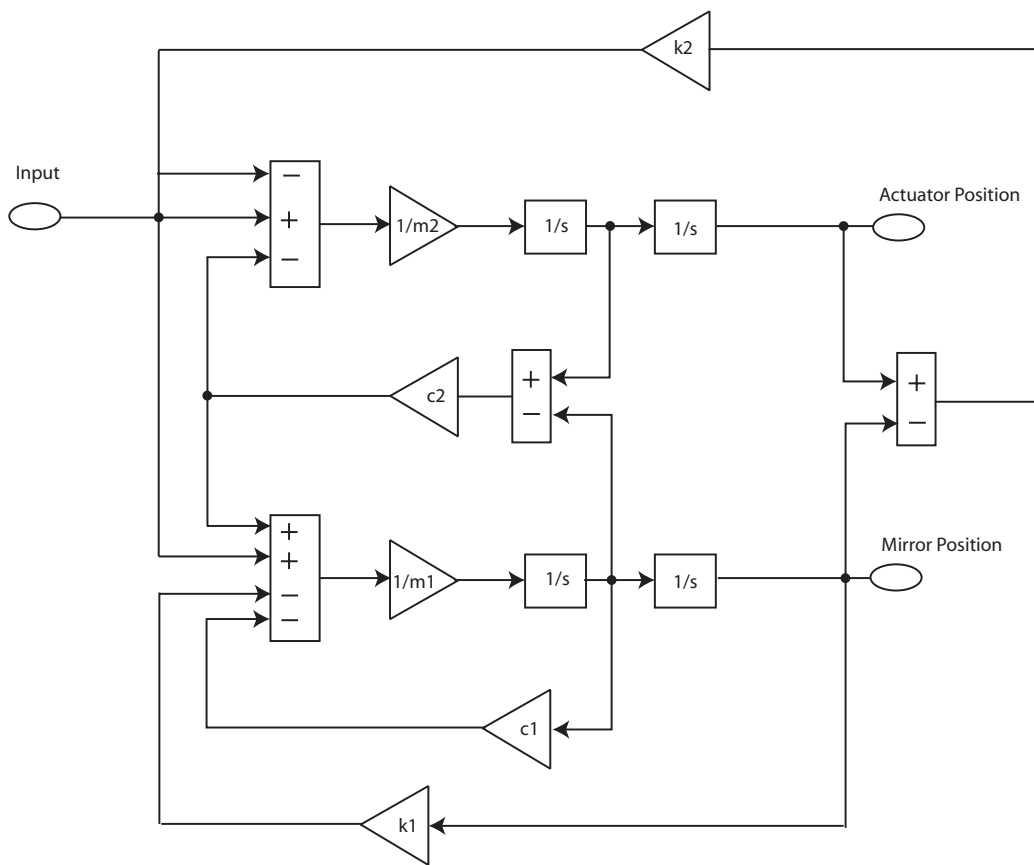


Fig. 8.4: Simulink model of the Actuator, vacuum cup and mirror.

Tab. 8.1: Actuator constants for the Simulink model.

Constants	Symbols	Values
Mass, actuator movable part	m2	8.5g
Spring, vacuum cup	k2	18000 N/m
Damping, vacuum cup	c2	5 Ns/m
Mass, mirror segment	m1	8g
Spring, mirror suspension	k1	11800 N/m
Damping, mirror suspension	c1	0.3994 Ns/m

9. MODEL VERIFICATION

To analyze the real process a "TR9404 Digital Spectrum Analyzer" was used. This instrument gives the possibility to get a transfer function of the system directly on the screen. After applying a signal with varying frequency to the actuator the transfer function can be observed on a screen. The values from that experiment have been plotted in Fig. 9.1 together with the model made previously. The experiment was made with the actuator in contact with a deformable mirror and the model that it is compared to is the complete model earlier described. The plot from this test is not exactly the same as the plot from the transfer function of the model. The resonance frequency for the two plots do differ but not much. The experiment with the stiffness of the vacuum cup was preformed just to get a rough model. Adjusting the stiffness value for the vacuum cup, based on the experimental data, will give a better model.

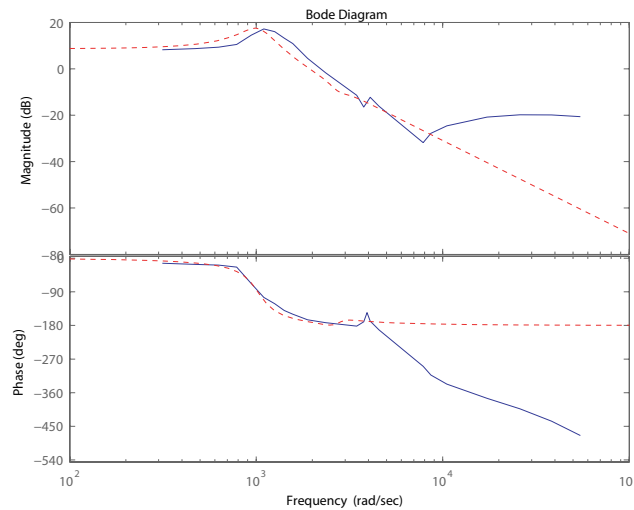


Fig. 9.1: Bode plot of actuator open loop *dashed line*=model, *continuous line*=real process.

In Fig. 9.2 the stiffness of the vacuum cup in the model has been adjusted and the model now corresponds to the real process. The figure is now

focusing more on what happens at lower frequencies and it is now possible to detect another difference between the two transfer functions. The gain is not constant for low frequencies as predicted. One hypothesis was that there was a plastic creep effect in the vacuum cup. A creep effect occurs when the rubber deforms with time without increasing pressure. This was tested in a small experiment and it showed that at a constant pressure the actuator did move with time. Another difference between the two Bode plots was found at about 5000 rad/sec. Some theories about what happens after 5000 rad/sec have been:

- **The system works like a servo system and the mass is decoupled at higher frequencies.** When a servo system decouples the mass at a certain frequency it results in an antiresonance and a resonance before the amplitude reaches the new level. The resonance could in this case have been filtered by the signal conditioner and therefore not be as visible as the antiresonance. After calculating the mass needed to be decoupled this theory were dismissed, it would be too large to be reasonable.
- **The rod in the actuator bends.** The vacuum connection to the cup causes asymmetry and could cause movement of the cup. This was tested by making sure the rod could not bend but the phenomena remained.
- **Resonance of the complete structure.** This theory was tested by attaching extra weight on the structure that holds the actuator. The resonance should have changed if this was the cause and it should be visible in the Bode plot. The resonance in the Bode plot was unchanged and thereby the theory was dismissed.
- **The signal conditioner affects the measurements.** There are several possible explanations for the disturbance.
 1. The signal conditioner could affect the measurements if the low-pass filters were designed with a too low cut-off frequency.
 2. Cross talk occurs between the oscillation circuit and the output.
 3. The modulation of the excitation frequency and the input signals frequency gives a unwanted affect at frequencies close to the excitation frequency.

The low-pass filters have been analyzed and they should not affect the measurements. The effect of modulation of the two signals was

calculated and the conclusion was that it could not have caused by this problem (see Chapter 6.4). Crosstalk on the signal conditioner circuit is not desirable but that is another problem and should not result in this behavior. At the output the 20 kHz signal remains high even after the low pass filters. In order to test the signal conditioner circuit the cable between the LVDT output and the input of the circuit was removed. The input was then connected to ground and an experiment was made again. The noise decreased and the conclusion at this stage was that the noise occurred before the signal conditioner circuit.

- **Noise transferred from voice coil to LDVT.** The theory was that the receivers in the LVDT received more of the signal from the voice coil as the frequency increased. At some point the signal from the voice coil dominates over the signal caused by movement from the rod. A first experiment to verify if this was the reason for the noise, was to remove one connection pin to break the connection between the voice coil and the LVDT. If the LVDT could register a movement this would indicate that there was some crosstalk. This experiment was made and the LVDT did register movement. Next experiment was to move the voice coil away from the LVDT and see if the noise disappeared when distance increased. Even a quite large distance gave no effect, the noise still remained. This would indicate that the main problem is not crosstalk between the voice coil and the LVDT.
- **Common power supply for Voice Coil and LVDT gives unexpected errors.** The output signal from the signal conditioner consists of a large 20 kHz signal and a smaller signal with the same frequency as the system's reference signal. The 20 kHz signal seems to be some kind of cross talk between the oscillation circuit and the output, but the other signal should not be visible if the voice coil is motionless. The only electrical connection between the two systems are the ground point and the power supply. When connecting the synchronous detector input to ground the error disappeared, and it does not seem to come from the ground connection. After using two different power supplies, one for the LVDT and one for the voice coil, the error decreased but did not disappear.

After several experiments to determine the reason for the deviation between the model and the process, a new model was made with a cross-connection, where the input signal to the actuator gets added at the actuator output (see Fig. 11.4). The result of the simulation looked similar to the measured disturbance (see Fig. 9.3). The conclusion is that the reason that the model

and the process differ is crosstalk from the signal conditioner circuit. The source of the crosstalk problem has not been found but new LVDT electronics will be designed later on and the crosstalk could probably be decreased.

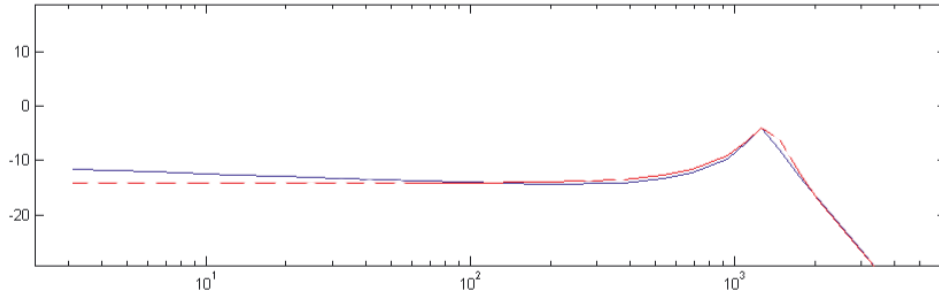


Fig. 9.2: Figure showing the plastic creep effect. *Dashed line*=model and *Continuous line*=real measurements.

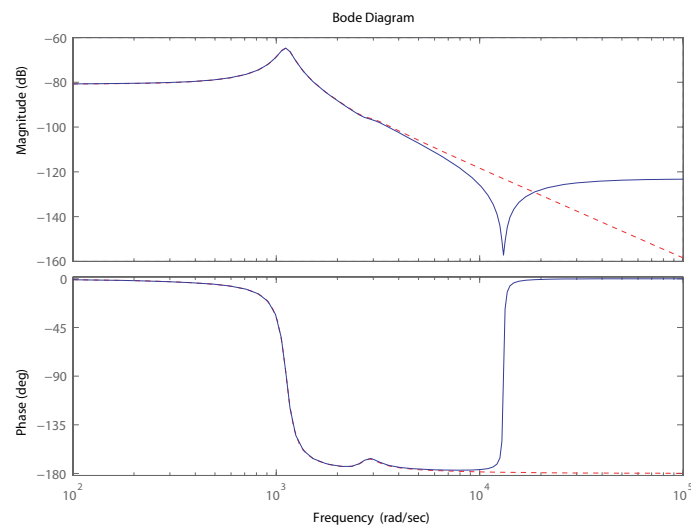


Fig. 9.3: Simulation of open loop response with (continuous line) and without (dashed line) crosstalk influence.

10. CONTROLLER

By looking at the Bode plot of the system a controller has been designed to make the system stable with a satisfying bandwidth. The bandwidth needed is at least 500 Hz but a 1000 Hz bandwidth is desirable. The LVDT, that measures the movement of the rod in the actuator, has an excitation frequency of 20 kHz. This demodulated excitation signal is damped in the filters in the signal conditioning circuit of the LVDT. These filters can limit the bandwidth since they affect the phase for frequencies around the desired bandwidth.

The controller consists of an integrator part for lower frequencies to take care of stationary error. It is not a real integrator since it has a lower cut-off frequency, but this is to avoid problems at startup of the analog controller. Another solution would be to have a relay that resets the integrator before the controller startup. Since there is no velocity sensor in the actuator it is necessary to add a differentiator to increase the phase margin. To decrease high frequency noise there is a cut-off at about 3 kHz. The controller was designed like the one in Figure 10.1. The equations can be seen below in Eq.10.1 and Eq.10.2.

$$G_1(s) = \frac{\tau_2 s + 1}{\tau_1 s + 1}, \quad G_2(s) = \frac{\tau_3 s + 1}{\tau_4 s + 1}, \quad G_3(s) = \frac{1}{\tau_5 s + 1} \quad (10.1)$$

$$G_{total}(s) = G_1(s) \cdot G_2(s) \cdot G_3(s) \quad (10.2)$$

10.1 Analog Implementation

The controller has been made using analog active filters. The first filter is the integrator and is realized as a noninverting voltage amplifier (see Fig. 10.3A) with two time constants which determine the pole and zero placement. The integrator in this case has a pole at 1Hz and a zero at 20Hz. The time constant for the pole is $\tau = (R_1 + R_2)C_1$ (see Eq. 10.3) and the zero is determined by $\tau = R_2C_1$. By using the transfer function and the fact $\omega = 1/\tau$

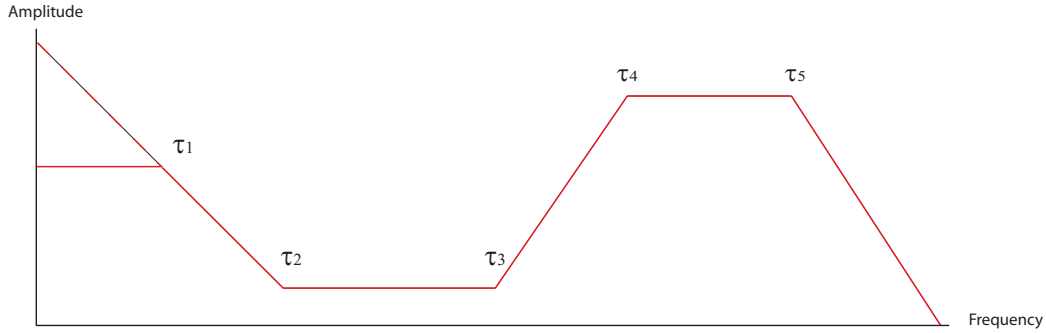


Fig. 10.1: Calculated Bode plot of the controller.

we get the values for R_1 , R_2 and C_1 . The other two resistors (R_3 and R_4) give the amplification of the stage ($A_f = 1 + \frac{R_3}{R_4}$).

The middle filter is a derivative and is implemented as an inverting active filter (see Fig. 10.3B). In this filter the time constant $\tau = R_2C_2$ gives the pole and $\tau = R_1C_1$ the zero (see Eq. 10.4).

$$\begin{cases} V_{in}(s) = R_1 + R_2 + \frac{1}{sC_1} * I \\ V_{out}(s) = R_2 + \frac{1}{sC_1} \\ H(s) = \frac{s + \frac{1}{R_2C_1}}{s + \frac{1}{(R_1+R_2)C_1}} \end{cases} \quad (10.3)$$

$$H(s) = -\frac{Z_2}{Z_1} = -\frac{\frac{\frac{1}{sC_2}R_2}{\frac{1}{sC_2}+R_2}}{\frac{\frac{1}{sC_1}R_1}{\frac{1}{sC_1}+R_1}} = \dots = -\frac{R_2}{R_1} * \frac{s + \frac{1}{R_1C_1}}{s + \frac{1}{R_2C_2}} \quad (10.4)$$

The last filter (see Fig. 10.3C) is another integrator to dampen high frequency noise that could interfere with the controller. This filter is designed in the same way as the previous one except for the lack of a zero. The transfer function looks like the one in Eq. 10.4 but with only a one in the numerator.

By using the spectrum analyzer the characteristics of the combined analog filter was analyzed. The result is plotted in Fig. 10.2.

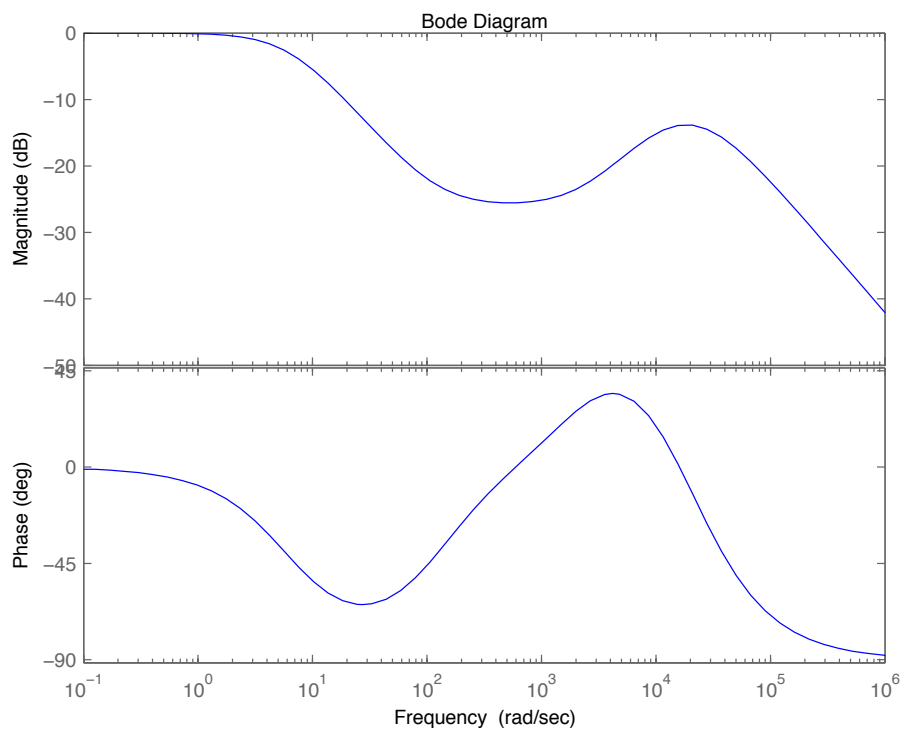


Fig. 10.2: Measured Bode plot of the analog controller.

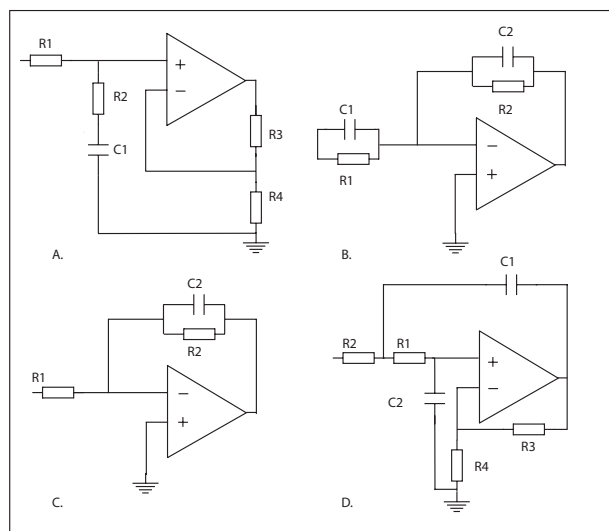


Fig. 10.3: The different building blocks in the analog controller. [A=Noninverting integrator (input step), B=Differentiator, C=Inverting low pass filter (final step), D=Sallen-Key low pass filter.]

10.2 Alternative Filter

The differentiator earlier described was easy to use, but to achieve more phase margin it is possible to use a state variable filter. It has the feature to change the Q-value for the filter [1].

By using a state variable filter an equation like Eq. 10.5 can be represented. The transfer function has to be transformed to state space representation Eq. 10.6.

$$G(s) = \frac{b_2 s^2 + b_1 s + b_0}{a_2 s^2 + a_1 s + a_0} \quad (10.5)$$

$$\dot{z} = Az + Bx \quad (10.6)$$

$$\dot{y} = Cz + Dx$$

$$A = \begin{pmatrix} m_{11} & m_{12} \\ m_{21} & m_{22} \end{pmatrix}, B = \begin{pmatrix} 1 \\ 0 \end{pmatrix}, C = \begin{pmatrix} n_{11} & n_{12} \end{pmatrix}, D = \begin{pmatrix} r_{11} \end{pmatrix}$$

The filter can then be realized as a canonical diagram (see Fig. 10.4), which can be converted to an analog circuit Fig. 10.5. OP-Amps U1 and

U2 in the analog circuit work as integrators. In the first integrator the three input signals have different gain depending on the resistor values R1, R2 and R3. The gain is determined by the equation $A_f = -\frac{1}{R_x C_1}$. The next integrator works in the same way, R4 and C2 determine the gain. All of the parameters from the canonical diagram are realized as the gain in the different steps. In this filter configuration the parameters m_{11}, m_{12}, n_{11} and n_{12} become negative. To get the right values for these parameters an inverter is needed, that is why the third amplifier U3 is used. The gain A_f of OP-amp U3 is chosen to get to get a reasonable output and avoiding saturation.

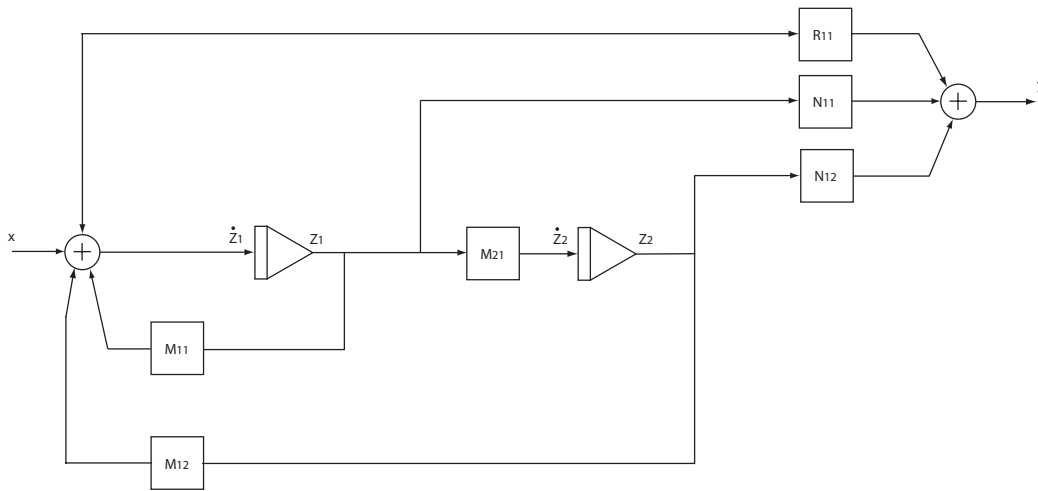


Fig. 10.4: Canonical diagram of the state variable filter.

The parameter m_{11} is determined by (R3,C1) together with (R1,C1). Parameter m_{12} is realized in the same way with (R2,C1) together with the gain in the loop. The three signals added in U4 have different scaling and that scaling corresponds to the values of r_{11} , n_{11} and n_{12} . In the analog circuit r_{11} is determined by (R7,R10). Parameter n_{11} is determined R8,R10 together with the output gain of amplifier U1. n_{12} is chosen in the same way.

The three resistors that give the right scaling are very sensitive to variation. To get as exact value as possible variable resistors was used. If only one of the resistors varies by $\pm 10\%$ there is a drastic change of the filter properties.

All amplifiers have a supply voltage of $\pm 15V$ and the output voltages are limited to that value. To be sure that no amplifier will saturate, a plot can be made to see when the output for the different stage reaches its highest value. The resistors and capacitors have been chosen so that saturation can be avoided for reasonable value at input.

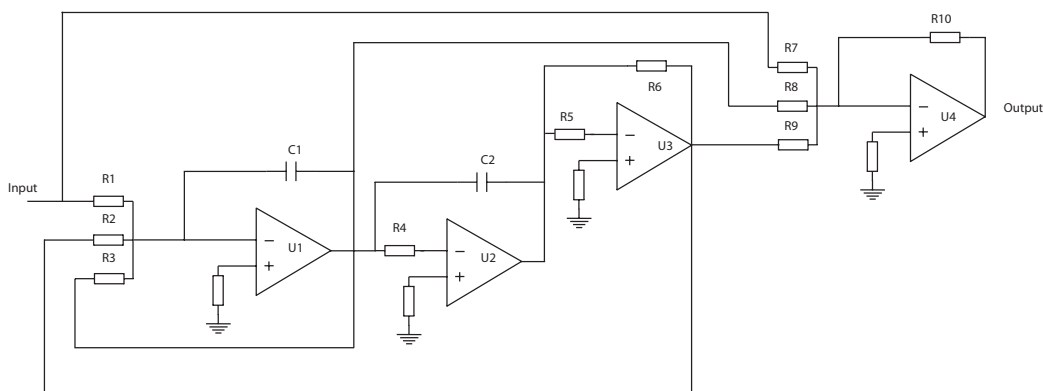


Fig. 10.5: Analog state variable filter

The state variable filter was tested and it works but showed to be too sensitive to use right now. With more exact capacitors and resistors this filter should work and help to get a better phase margin. After experimenting with this filter for a while we chose to go back to the filter earlier described. If it turns out later that a filter with variable Q-value is needed to get enough phase margin this filter could be used.

10.3 Sallen-Key Filter

A Sallen-Key filter is an active filter configuration with the advantage to choose Q-value without the use of inductors. In the construction of the signal conditioner circuit, a second order low-pass filter is used. As earlier described the filter had to be redesigned to get a sufficient bandwidth. The new bandwidth was 3 kHz. In this case we concentrated on replacing the capacitors, to make as few changes as possible. To calculate the new values equation 10.7 and 10.8 were used together with table 10.1. The table gives examples of how to choose the values for Butterworth and Bessel filters. Butterworth is less damped but has also less affect on the phase for frequencies lower than the cut-off frequency. For the second order filters the difference is quite small between the two filter type, but in this application a Butterworth filter was chosen. The amplification A_0 of the filter is chosen by two resistors R_3, R_4 . If Bessel or Butterworth is not desirable it is easy increase or decrease the damping by changing the Q-value.

$$A(s) = \frac{A_0}{1 + \omega_c [C_2 (R_1 + R_2) + (1 - A_0) R_2 C_1] s + \omega_c^2 R_1 R_2 C_1 C_2 s^2} \quad (10.7)$$

$$\begin{cases} A_0 = 1 + \frac{R_3}{R_4} \\ a1 = w_c C_2 (R_1 + R_2) + w_c (1 - A_0) R_2 C_1 = \frac{\omega_c}{Q} \\ b1 = w_c^2 R_1 R_2 C_1 C_2 = \omega_c^2 \end{cases} \quad (10.8)$$

$$Q = \frac{1}{2\xi} \quad (10.9)$$

Tab. 10.1: Second-order Filter Coefficients

Coefficients	Bessel	Butterworth
a1	1.3617	1.4142
b1	0.618	1
Q	0.58	0.71
A_0	1.268	1.568

11. POTENTIAL USE OF AN OBSERVER

This section has been written in collaboration with supervisor Torben Andersen.

In the article "Resonant Load Control Methods for Industrial Servo Drives" [6] the authors discuss a velocity observer for use in electrical motors. The observer in the article is called "Rigid-body Luenberger observer" and can be seen in Fig. 11.1. When using the observer the controller can be redesigned. In the previously discussed controller, a compensation network with a differentiator was used. The differentiator was needed to compensate for the phase lag caused by the lack of velocity information. The observer is used to estimate the velocity and that information gives the possibility to design a cascade controller. A block diagram for the new controller is found in Fig. 11.2. The inner loop in the cascade controller is made faster than the external loop. The observer is designed with a bandwidth to prevent it from interacting with the system. A comparison, between the previous controller and the new controller with observer, is made in Fig. 11.3. As seen in the figure there is a gain in the phase at higher frequencies for the new controller. This makes it possible to control the actuator without amplifying noise.

In the writing moment the observer has not been finished yet but the electrical design is in process. The Simulink design can be found in Fig. 11.4.

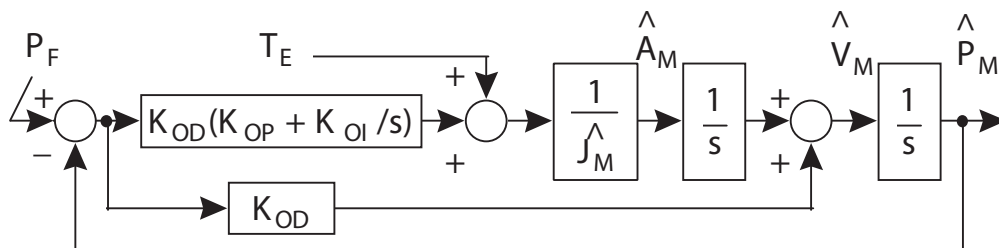


Fig. 11.1: Extended rigid-body Luenberger observer (from [6]).

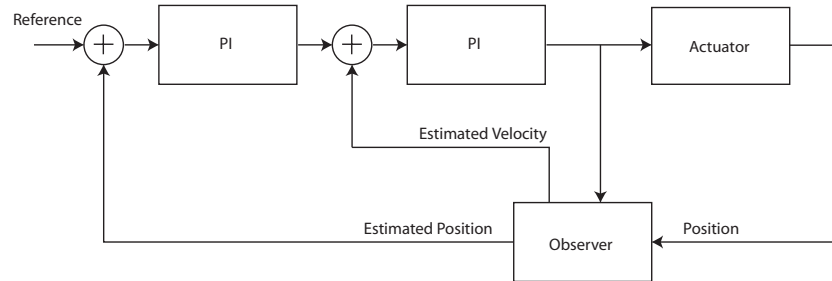


Fig. 11.2: Block diagram of the controller including observer.

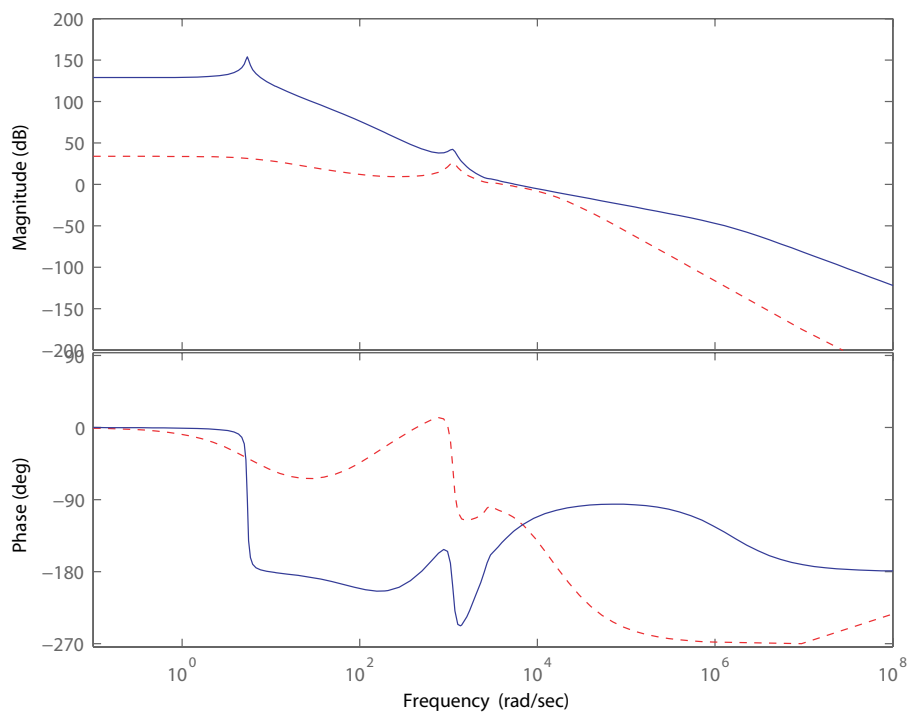


Fig. 11.3: Comparison of open loop Bode plot with and without observer. *Continuous line*=with observer, *dashed line*=without observer.

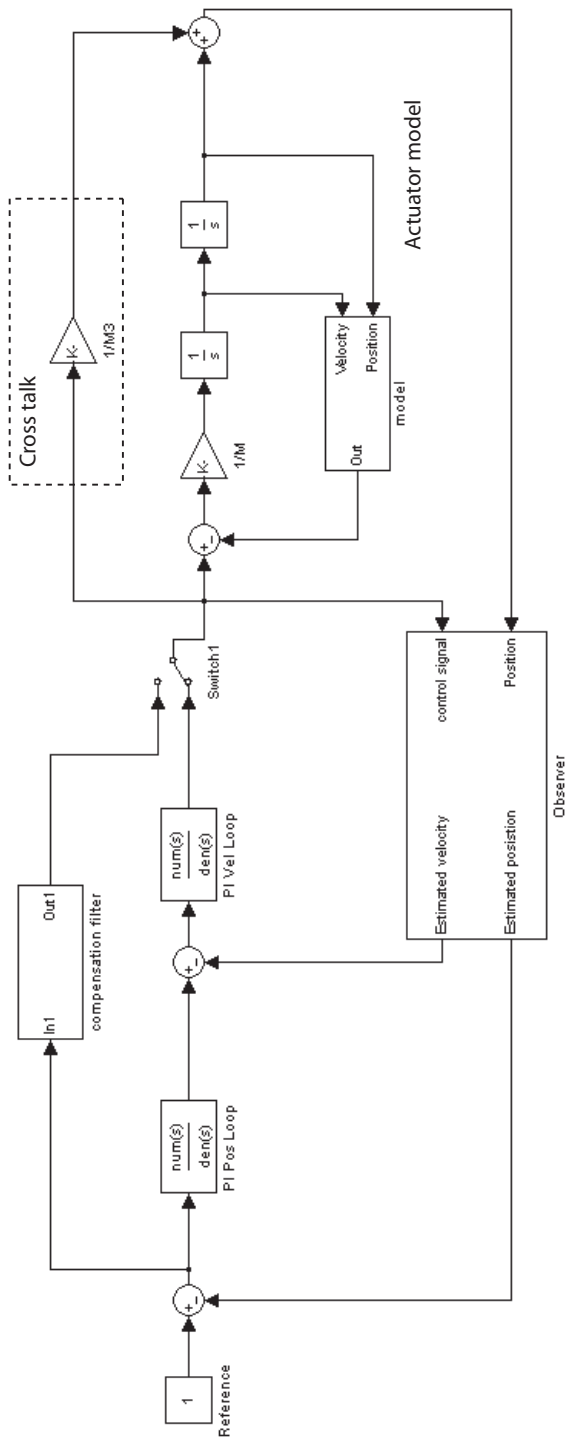


Fig. 11.4: Simulink model of the system, including observer.

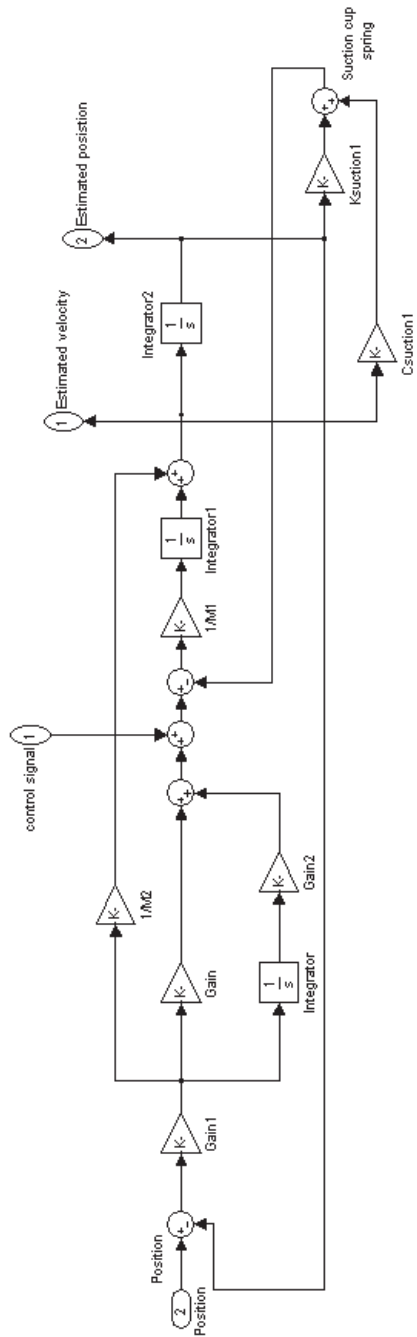


Fig. 11.5: Simulink model of the observer block from Fig. 11.4.

12. CONCLUSION AND SUGGESTIONS OF FUTURE WORK

The goal for this thesis has been to get an actuator that can deform a mirror tens of micrometers with a accuracy about 100 nanometers. In the same time the actuator has to be quite fast and have at least a bandwidth of 500Hz, it would be desirable to increase this bandwidth to 1000Hz. After several experiments it became clear that it would be impossible to get satisfactory results with the experiment setup. The noise visible at the output from the LVDT electronics was amplified too much in the controller. If the noise could be decreased enough, a bandwidth of $\approx 300\text{Hz}$ could have been possible, but to get a higher bandwidth the controller needed to be redesigned. The reason to use the differentiator is that the velocity in the voice coil is unknown. To be able to remove the differentiator, the velocity has to be known either by measuring or by estimating. When using the velocity for feedback the phase will only be -90° , instead of the -180° as for position feedback. Thereby there is no need for the differentiator to increase the phase. A velocity sensor demand a new design of the actuator. Building a new actuator is right now seen as a last resource. By using an observer it would be possible to estimate the velocity in the voice coil and use that information in the feedback. If the velocity is known, two PI-controller can be used in a cascade controller and the D-part is unnecessary. Another problem found in the experiments was cross-talk in the LDVT electronic circuit. A new electronic circuit will be designed to decrease the cross talk. When using the observer the signal from the LVDT is filtered in a lowpass filter with 300 Hz cut-off frequency, thus the cross talk signal at 20 kHz is not a big problem anymore. The LVDT electronics will have to be redesigned anyway since the circuit used has been altered a couple of times and right now is only a version for laboratory use. In the future, experiments will be done with a bigger mirror with several actuators and then a standard circuit needs to be used.

BIBLIOGRAPHY

- [1] *State Variable Filter Design for Audio Applications*, 2000. URL: <http://www.uwm.edu/People/msw/StateVariable/> (accessed November 9, 2004).
- [2] *Euro50*, 2004. URL: <http://www.astro.lu.se/~torben/euro50/> (accessed November 9, 2004).
- [3] Analog Devices. *Universal LVDT Signal Conditioner*, 2003.
- [4] Torben Andersen et al. *Euro50, A 50 m Adaptive Optics Telescope*. Lund Observatory, 2003.
- [5] Fredrik Bjöörn and Olof Garpinger. Modeling and control of a large deformable mirror. Master's thesis, Department of Automatic Control, Lund University, Sweden, Mars 2005.
- [6] George Ellis and Robert D Lorenz. Resonant load control methods for industrial servo drives, 2000. *IEEE Industry Applications Society*, Annual Meeting, Rome, Italy October 2000.
- [7] John W. Hardy. *Adaptive Optics for Astronomical Telescopes*. Oxford University press, New York, 1998.
- [8] Macro Sensors. *Instruction Manual DC-Operated LVDT signal conditioner Model DCM-1000*, 2000.
- [9] McGhee. *Linear Actuator*. BEI Kimco Magnetics Division, 2003.
- [10] Philips Semiconductors. *LVDT signal conditioner NE/SA/SE5521*, 1994.
- [11] Zahid Rahim. *Using the NE5521 signal conditioner in multi-faceted applications*. Philips Semiconductors, 1988.
- [12] Olof Sandberg. Control of the Euro50 Secondary Mirror Cell. Master's thesis, Department of Automatic Control, Lund University, Sweden, Mars 2005.

- [13] Texas Instruments Incorporated. *High-Voltage, High-Current OPERATIONAL AMPLIFIER*, 2003.